Pergamon

Ocean Engng, Vol. 23, No. 8, pp. 667–689, 1996

0029–8018/96 $15.00 + 0.00

0029–8018(95)00066-6

ASSIMILATION OF ALTIMETER WAVE HEIGHT DATA INTO A SPECTRAL WAVE MODEL USING STATISTICAL INTERPOLATION

I. R. Young* and T. J. Glowacki†

*Dept. Of Civil Engineering, University College, University of New South Wales, Canberra, A.C.T., Australia (e-mail: i-young@adfa.oz.au);
†BMRC, GPO Box 1289K, Melbourne, VIC 3001, Australia (e-mail: tzg@tracy.ho.bom.gov.au)

(*Received* 7 *July* 1995; *accepted in final form* 1 *September* 1995)

Abstract—A scheme for the assimilation of altimeter wave height data into a second generation wave prediction model is developed. The scheme modifies the model wave spectrum so as to be consistent with the satellite observed values of significant wave height. This modification is achieved, however, so that the adjusted wave field is consistent with the model physics and the forcing wind field. In this manner the modifications to the wave field persist in the model, thus yielding long term improvements in model performance. In addition, a statistical interpolation scheme is used to ensure that maximum use is made of the point observations made by the satellite. In this manner, not only points directly beneath the satellite track are updated. Points adjacent to the track are also modified, the extent of this modification depending on the spatial correlation of the wave field. The scheme is applied to a computationally efficient second generation wave model. The improvement in performance is significant, demonstrating that assimilation may be a very efficient alternative to proceeding to more sophisticated and expensive third generation models. This is particularly true where the forcing wind field may be of poor quality. The results also demonstrate that with the addition of assimilation, relatively small computational grids can be utilized. Swell generated external to the grid will be included through the assimilation cycle.

1. INTRODUCTION

In the approximately 40 years since the advent of the first spectral wave prediction models (Gelci *et al.*, 1957; Barnett, 1968; Ewing, 1971), the accuracy and reliability of such models have increased enormously. This has largely been achieved as a result of an improved understanding of the physical processes responsible for wind wave evolution. This improved physical understanding has been incorporated in progressively more sophisticated models, thus improving model performance. This continued development process, however, exhibits diminished returns: the added computational expense of a more sophisticated model yielding only a marginal increase in model performance. In addition, there are external parameters influencing model performance which will not be affected by refined physics. An example of this is the quality of the wind fields used to drive the wave model. Even the most sophisticated wave model will yield poor results if forced by poor quality wind fields.

One possible means of improving model performance within such constraints is to assimilate measured data into the model. These data could be in situ, measured with conventional instruments such as wave buoys or remotely sensed by orbiting satellites. The much greater spatial coverage obtained from satellites favours this data source.

This paper describes a process for assimilating data from the GEOSAT radar altimeter into a wave prediction model. The adopted technique modifies the model spectral wave field so as to be both consistent with the observed altimeter data and in dynamic equilibrium with the imposed wind field. In addition, a statistical interpolation (SI) scheme is used to make maximum use of the observed wave information.

The arrangement of the paper is as follows. In Section 2 a review of data assimilation schemes utilized or proposed for wave models is presented. Section 3 describes the method adopted for the modification of the model wave spectrum within the constraints of the wave model. The SI scheme used to take maximum advantage of the observed altimeter data is briefly described in Section 4 (full details are contained in Appendices), followed by an application and validation of the full assimilation scheme in Section 5. Conclusions of the study are presented in Section 6.

2. DATA ASSIMILATION METHODS

One of the first published attempts at the assimilation of wave height data into a wave prediction model was made by Komen (1985). He investigated the case of swell propagating from a generation region in the Norwegian Sea to a measurement point at the entrance of Rotterdam harbour. The prediction of the swell at Rotterdam harbour using the GONO model (Janssen *et al.*, 1984) was significantly higher than measured. Updating the model with measured buoy data at a point approximately 500 km north of the measurement site significantly improved the model swell prediction for this event.

Thomas (1988) proposed the first scheme to update the full wave spectrum using buoy measurements of significant wave height and wind speed. A JONSWAP parameterization was assumed for the wind–sea part of the spectrum, which was then updated by using the buoy wind speed to re-scale the energy and peak frequency (maintaining its 'wave age'). The remaining swell part of the spectrum was updated by changing only the energy scale. This technique yielded promising results, indicating that operational wave data assimilation schemes may become feasible.

Hasselmann *et al.* (1988) and Bauer *et al.* (1992b) made the first attempt at the global assimilation of satellite data, using SEASAT altimeter wave height data for a 30 day period in August, 1978. Their update scheme simply changed the scale of the model spectrum,

$$F_{new}(f,\theta) = \gamma F_{model}(f,\theta) \tag{1}$$

where $F_{new}(f,\theta)$ is the new or modified spectrum, $F_{model}(f,\theta)$ is the initial model spectrum, f is frequency and θ the propagation direction. The scale factor γ is proportional to the square of the ratio between the altimeter wave height and the model first-guess wave height. The scaling had an extreme value at the sub-satellite altimeter measurement point and relaxed back linearly to unity at the boundary of some specified 'region of influence'. For a continuous one-month assimilation experiment, good results were achieved using a region of influence of 9° x 9°. The assimilation scheme was successful in updating regions dominated by swell, yielding globally averaged correction decay times of the order of five days, but had little impact on the wind–sea, which reverted rather rapidly to an equilibrium corresponding to the uncorrected local wind. It was concluded that the improvement of the wind–sea predictions would require a scheme which also corrected the erroneous wind forcing.

This problem was addressed by Janssen *et al.* (1989), who used altimeter wave height data to introduce corrections to both the wave and wind fields. Their scheme firstly partitioned the spectrum into wind–sea and swell, the swell being defined as the region of the spectrum in which the atmospheric input source term was zero. The swell spectrum was modified by a change of the energy scale, maintaining its shape and peak frequency, while the wind–sea part of the spectrum was modified in a manner similar to that of Thomas (1988), using JONSWAP duration limited growth relationships. Introducing the additional assumption that the energy of the wind–sea and swell were changed by the same factor, a new wind–sea and swell spectrum were then determined. At the same time the wind speed (or friction velocity u_*) was corrected to conform with the new wind–sea. This information was then distributed to surrounding grid points, as in Hasselmann *et al.* (1988), but using in this case a correlation region of only one wave model grid square (3° x 3°). Although both the wind and sea state had now been adjusted, only relatively short correction decay times of the order of one day were achieved. This was presumably largely due to the much smaller region of influence used. If the scale of the region of influence is significantly smaller than the spacing between successive ascending or descending satellite orbits (~25° longitude), only a small fraction of the ocean is corrected in one day's sweep of the satellite over the ocean. Wave energy from uncorrected regions between the satellite tracks can then propagate into the corrected regions and degrade the quality of the updated regions.

Lionello *et al.* (1992) proposed a modification of the scheme of Janssen *et al.* (1989) using alternative scaling relations. When swell leaves a generation region, it initially has a relatively large steepness characteristic of a wind–sea. However, linear dispersion and the nonlinear processes of dissipation and energy transfer, which are both strongly dependent on the wave steepness, rapidly reduce the steepness to a level where all the source terms become negligible. If the wave height is under predicted by the model (which was normally the case for the SEASAT studies) the assimilation schemes mentioned above all increase the swell steepness. This immediately activates the dissipation and nonlinear source terms, causing the wave energy to decrease again. In the re-scaling scheme of Lionello *et al.* (1992), both the amplitude and the frequency of the swell are altered such that the swell steepness is maintained during the assimilation process. By this modified method the correction decay times were increased significantly, and are now of the order of the propagation times of swell across ocean basins.

The above schemes are all relatively simple and exhibit a number of shortcomings. All require rather *ad hoc* assumptions for the separation of wind–sea and swell, which are treated separately in the assimilation scheme. Similarly, the wind–sea part of the spectrum is updated by applying JONSWAP shape or scaling relations. The altimeter wave height measurements are assumed to be representative over some arbitrary distance adjacent to the satellite ground track. The 'laterally spread' observations are then incorporated into the model using simple 'blending' algorithms.

A more fundamental approach to the problem would involve fitting the model prediction to the observations by modifying the model control variables, i.e. the wind field, rather than the model output. A general solution to this type of problem is given by the adjoint model formalism (Marchuk, 1974; Le Dimet and Talagrand, 1986). Adjoint wave models have been developed and successfully applied to assimilate wave data in simple test cases (De Valk and Calkoen, 1989; De las Heras and Janssen, 1992). However, operational implementation of such an approach appears to be computationally very costly and its feasibility is yet to be determined.

Formally, the change in the wind field needed to produce a given change in the wave field can be determined by inverting the wave model. However, this is normally an even more expensive computation. The basic concept of the adjoint model approach is to determine changes needed in the control variables to achieve a desired change in the model prediction without explicitly inverting the prognostic model operator.

Bauer *et al.* (1990, 1992a) have proposed an alternative assimilation method in which the wave transport equation operator is inverted. The central idea is to estimate the impulse response (Green's) function of the system which describes the balance of the spectral energy changes influenced by perturbations in the wind fields. This direct approach becomes computationally feasible, however, only by introducing approximations in the determination of the impulse response function. Tests for ideal cases show the method has merit but its application to 'real' data is yet to be assessed.

3. DYNAMIC SPECTRAL MODIFICATION

Satellite altimeter data consist of observations of the significant wave height, H_s whereas a spectral wave prediction model requires information on the full directional spectrum, $F(f,\theta)$. Hence, in an assimilation scheme in which the model wave spectrum is to be modified so as to be consistent with the observed altimeter data, no information on the shape of the observed spectrum is available. Only the integral spectral property, H_s is available. However, as reported in Section (2) the model places constraints on the possible shape of the spectrum. If corrections to the model spectrum are to persist within the model, they must be in dynamic equilibrium with the model winds. Should this not be the case, the spectrum will be quickly changed by the model so as to be in equilibrium.

This requirement was recognized by Lionello *et al.* (1992) and a scheme appropriate to a third generation wave model developed. In the present context, a computationally more efficient second generation model is adopted. Due to the differing physics in such a model, the dynamic constrains differ from a third generation model and hence the details of the dynamic spectral modification are also different.

The model adopted in the present study is the ADFA1 model of Young (1988). As with other second and third generation models, this model considers the source terms which are responsible for spectral evolution to be the sum of three processes

$$S = S_{in} + S_{nl} + S_{ds} \tag{2}$$

where S_{in} represents atmospheric input to the spectrum from the wind, S_{nl} accounts for the effects of nonlinear interactions between spectral components and S_{ds} the dissipation of energy by 'white-cap' wave breaking. In common with other second generation models, ADFA1 represents S_{ds} in terms of a 'saturation' spectrum. Any energy above this saturation limit is assumed to be dissipated by breaking. The saturation spectrum has the form

$$F_{\alpha}(f,\theta) = \alpha g^2 (2\pi)^{-4} f^{-5} D(\theta) \tag{3}$$

where D is a directional spreading function, assumed to be of the form $\cos^2\theta$ and α is a wave age dependent Phillips (Phillips, 1958) coefficient (Young, 1988)

$$\alpha = 0.0029\tilde{E}^{-0.2} \tag{4}$$

where $\tilde{E} = Eg^2/U_{10}^4$, $E = \int F(f,\theta) df d\theta$ is the total spectral energy and U_{10} is the wind speed measured at a reference height of 10m. Due to the negative exponent in (4) an increase in the total energy of the spectrum will result in a reduced value of α. Hence, any modification of the spectrum which results in a high frequency form not in agreement with (3) will be quickly modified by the model.

It is possible to modify the spectrum in a number of ways and still satisfy this high frequency constraint. The technique adopted here, and described below, attempts to do so without modification to the directional spreading.

The adopted spectral modification technique proceeds in a piecewise manner with differing techniques depending on whether the observed (altimeter) energy is greater than or less than the corresponding model energy.

Initially the observed (altimeter) energy, E_{obs} (or H_s) and the model energy, $E = \int F(f,\theta)dfd\theta$ are available. The ratio of these two values is

$$R = \frac{E_{obs}}{E} \tag{5}$$

3.1. *Observed energy greater than model energy: R >1*

(i) The model spectral energy is increased to match the observed altimeter energy whilst preserving the model spectral shape (Fig. 1a)

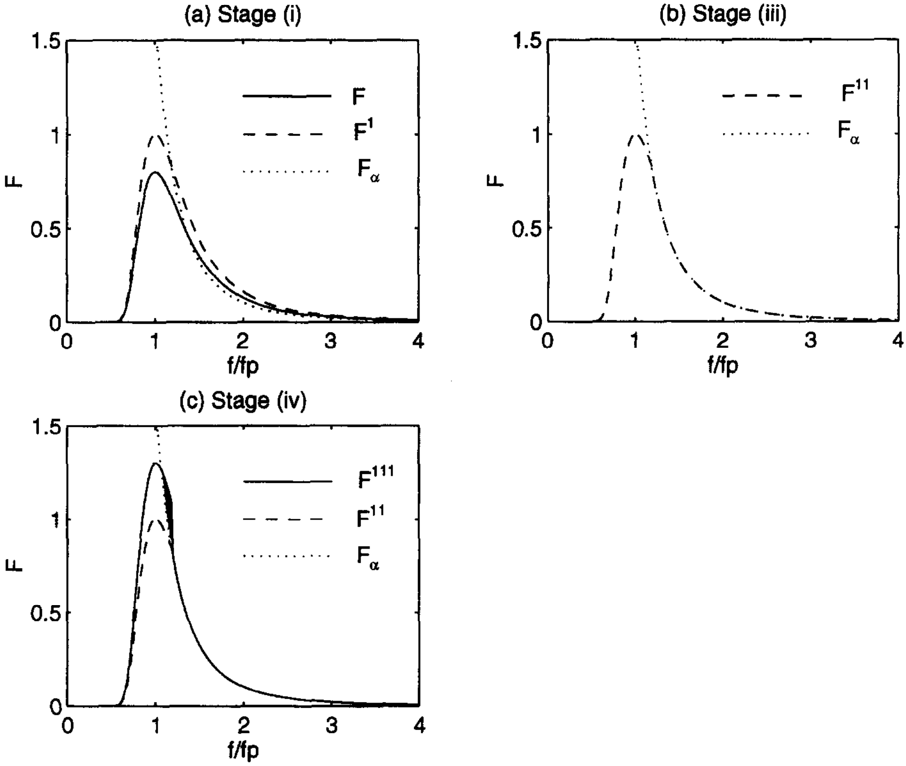

Fig. 1. The individual stages of the dynamic spectral modification scheme for the case where the observed energy is greater than the model energy, $R > 1$. The stages marked, (i), (iii) and (iv) correspond to those described in Section 3.1. The small shaded region in panel (c) is still above the saturation limit and will be corrected on the next iteration of the modification scheme.

$$F^{1}(f,\theta) = RF(f,\theta) \tag{6}$$

(ii) The spectrum is partitioned into two regions: frequency-direction components with energy equal to or greater than the saturation limit (3) are termed saturated (represented by subscript s) whilst components below this limit are termed non-saturated (subscript ns). The modified spectrum can then be represented as

$$F^{1}(f,\theta) = F^{1}(f,\theta)_{ns} + F^{1}(f,\theta)_{s} \tag{7}$$

(iii) Energy in F^{1} above the saturation limit as calculated from (3) with the observed energy E_{obs} is now dissipated yielding a modified spectrum $F^{11}(f,\theta)$ (Fig. 1b)

$$F^{11}(f,\theta) = F^{11}(f,\theta)_{ns} + F^{11}(f,\theta)_{s} \tag{8}$$

The total energy of F^{11} becomes $E^{11} = \int F^{11}(f,\theta)dfd\theta$ whilst that of the spectrum at stage (i) above is $E^{1} = E_{obs} = \int F^{1}(f,\theta)dfd\theta$. Due to the energy that was dissipated in stage (iii), $E^{11} \leq E_{obs} = E^{1}$. The difference between these quantities, $\Delta E = E^{1} - E^{11}$, represents the energy dissipated in stage (iii).

(iv) The energy dissipated in stage (iii), ΔE, is now redistributed to the non-saturated components of F^{11}. The total energy in these non-saturated components is $E^{11}_{ns} = \int F^{11}(f,\theta)_{ns}dfd\theta$. The energy of these components is increased whilst maintaining the directional spreading using the relationship (Fig. 1c)

$$F^{111}(f,\theta) = R_{1}F^{11}(f,\theta)_{ns} + F^{11}(f,\theta)_{s} \tag{9}$$

where

$$R_{1} = \frac{E^{11}_{ns} + \Delta E}{E^{11}_{ns}} \tag{10}$$

The energy redistribution process of stage (iv) may now have raised some energy above the saturation level (Fig. 1c). To account for this, the process returns to stage (iii) and is repeated until no further modification to the spectrum occurs.

3.2 *Observed energy less than model energy*: $R < 1$

(i) The original model spectrum is again partitioned into saturated and non-saturated sections

$$F(f,\theta) = F(f,\theta)_{ns} + F(f,\theta)_{s} \tag{11}$$

where the saturation level is based on the total energy of the original model spectrum, E (Fig. 2a).

(ii) The non-saturated components in (11) are now raised to the new saturation level determined from (3) and based on the observed altimeter energy, E_{obs} (Fig. 2b). The resulting spectrum becomes

$$F^{1}(f,\theta) = F(f,\theta)_{ns} + F^{1}(f,\theta)_{s} \tag{12}$$

The total energy of F^{1} is $E^{1} = \int F^{1}(f,\theta)dfd\theta$ and since the saturated components of this spectrum were increased relative to the original model spectrum, F: $E^{1} > E > E_{obs}$. The amount of energy added to the spectrum in raising the saturated components to the new

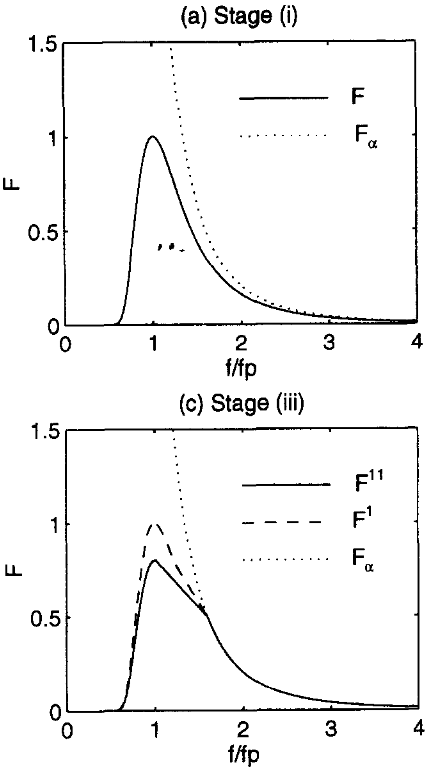

Fig. 2. The individual stages of the dynamic spectral modification scheme for the case where the observed energy is less than the model energy, $R < 1$. The stages marked, (i), (ii) and (iii) correspond to those described in Section 3.2.

saturation level is $\Delta E = E^1 - E$. The total energies of the saturated and non-saturated portions of F^1 become respectively, $E_s^1 = \int F^1(f,\theta)_s df d\theta$ and $E_{ns}^1 = E_{ns} = \int F(f,\theta)_{ns} df d\theta$. The total energy in the new saturated region of the spectrum can also be represented as $E_s^1 = E + \Delta E - E_{ns}$.

(iii) The spectrum F^1 falls into one of two classes.

(a) $E_s^1 > E_{obs}$. In this case the energy in F^1 is reduced by commencing at the lowest frequency band and moving to higher frequencies, progressively setting $F^1(f, \theta)$ to zero until $E^1 = E$.

(b) $E_s^1 < E_{obs}$. In this case the energy of the non-saturated components are reduced whilst maintaining the directional spreading of these components (Fig. 2c)

$$F^{11}(f,\theta) = R_2 F(f,\theta)_{ns} + F^1(f,\theta)_s \tag{13}$$

where

$$R_2 = \frac{E_{obs} - E_s^1}{E_{ns}} \tag{14}$$

4. APPLICATION OF STATISTICAL INTERPOLATION TO SATELLITE WAVE DATA

Statistical interpolation is widely used in data assimilation systems and a number of techniques employing SI have been presented in the meteorological literature. The basis of SI derives from the Gauss–Markov theorem and was first presented by Gandin (1963). Since it is less well known in Engineering, the mathematical description of SI (after Lorenc, 1981) as applied to the present application appears in Appendix A. The specific aspects of the assimilation problem dealt with in this paper are:

(i) one variable of concern, H_s;
(ii) a two dimensional grid of relatively small domain;
(iii) the source of observational data and it's specific characteristics and configuration.

It is thus a univariate, two dimensional version of SI that has been applied here. It performs two important tasks in the process of assimilation of H_s into the wave model.
(i) quality control of altimeter data by the method of cross-validation;
(ii) analysis (or inclusion in model) of H_s data validated in (i) over the wave model grid and with the model prediction as a first guess.

The analyzed wave field is the one which enters the assimilation cycle by replacing the original model field used in the SI as a first guess.

The strategy for using SI in this context has been specifically tailored to the configuration of the altimeter data, their quantity and the relatively small grid domain and dimensions. No splitting of the computational domain into overlapping data checking/analysis subdomains as commonly done in other SI applications has been attempted here. The analysis subdomain is identical to the whole grid domain and thus each datum is allowed (theoretically) to cross-check any other datum and to influence analysis of every grid point through the SI.

Raw altimeter data produced by orbiting satellites are often erroneous with observations of both unrealistic values and positions. To prevent such observations from entering the assimilation cycle a provision for a two stage quality control has been implemented. This consists of an initial check for the gross error against the given guess field and is followed by a cross-validation check for consistency with other nearby data which uses SI (Appendix B). In the initial check an observation is flagged as 'suspect' when its normalized deviation from prediction is greater than four standard deviations (Lorenc, 1981) (see Appendix B).

In the cross-validation stage all suspect data are excluded from checking other data. All data however, whether suspect or not undergo checking and in the process they are classified into two categories 'valid' or 'invalid'. When a datum is classified as 'invalid' it is excluded from checking other data, and is not used in the following analysis stage.

Normalized deviations of H_s from the first guess field are analyzed over the grid domain using the SI application described in Appendix C. It is common practice that the application of SI is proceeded by an observational data selection so that not necessarily all data are used at once. This is aimed at increasing computational efficiency by reducing the size of the covariance matrix and eliminating the possibility of an ill-conditioned matrix. This usually takes the form of specifying the radius (with respect to the analysis domain centre) from which data are taken to influence the data-checking/analysis domain and of replacing closely spaced data with 'super observations'. One of characteristics of the data used here is that, for a given satellite pass, altimeter data of concern form a ground track which is approximately a straight line and that they fall within a time interval of a few minutes. Consequently, data selection is based on ordinal (time followed) numbering of H_s observations. Indexed data are selected, checked and deviations analyzed k times for the whole grid domain and each time, with every l^{th} datum selected for use by the SI scheme. The final H_s analysis is the average of the partial data analyses of deviations, renormalized and added to the first guess. Parameters k and l are user specified, but were set here to exhaust all available data in a reasonable (work station) time. Each pass typically consists of a few hundred observations and this was not excessive to analyze all at once. Splitting the observations into groups, however, produced faster execution without a noticeable difference in accuracy. Though closely spaced, altimeter data are hardly likely to lead to an ill-conditioned covariance matrix because they are also evenly spaced. Thus, no replacement of data by 'super observations' was performed here and the possible problems avoided by the application of a highly accurate method (Schnabel and Eskov, 1990) for the factorization/inversion of the covariance matrix.

In the absence of detailed knowledge of the wave model (first guess) error correlations, and because they are subject to change in the feedback process of data assimilation they were initially assumed to be approximated by a gaussian shape correlation formula:

$$<\pi_i \pi_j> = \exp[-1/2(r_{ij}/s)^2] \tag{15}$$

where r_{ij} is the distance between two points of the guess field and s is a length scale parameter (currently set at 350 km). A better approximation to the value of s will be determined after more information is gathered on the performance of the data assimilation scheme. Observation errors were assumed to be uncorrelated.

5. RESULTS FOR THE TASMAN SEA

5.1. *Details of study region*

As a test of the performance of the assimilation scheme a one month hindcast test for the Tasman Sea (between Australia and New Zealand) was conducted. The extent of the computational grid is shown in Fig. 3. The grid was rotated 15° clockwise from North so as to take maximum advantage of land masses in forming boundary conditions. With the exception of land boundaries, all other boundaries were of the radiation type (energy can leave the computational domain but none can enter). The relatively small spatial extent of the computational grid and the existence of radiation boundaries along its Southern edge means that much energy generated in the Southern Ocean will be excluded from the computations. Hence, one would expect the model to generally under predict. The need for a large computational domain so as to encompass remote generation sites is, in theory, not necessary if assimilation is utilized. Swell entering the computational domain will be 'seen' by the satellite and the model updated to reflect its presence. Hence, the small computational domain was selected to test the ability of the assimilation scheme to account for such effects. In addition, the grid selection ensures that model performance without assimilation will be poor, any improvement as a result of assimilation being easily seen.

The model utilized here is numerically unconditionally stable and a computational space step of 70km and a time step of 90 minutes were adopted (Young, 1988). The directional wave spectrum, F, was defined with 15 frequencies and 16 directions (a directional resol-

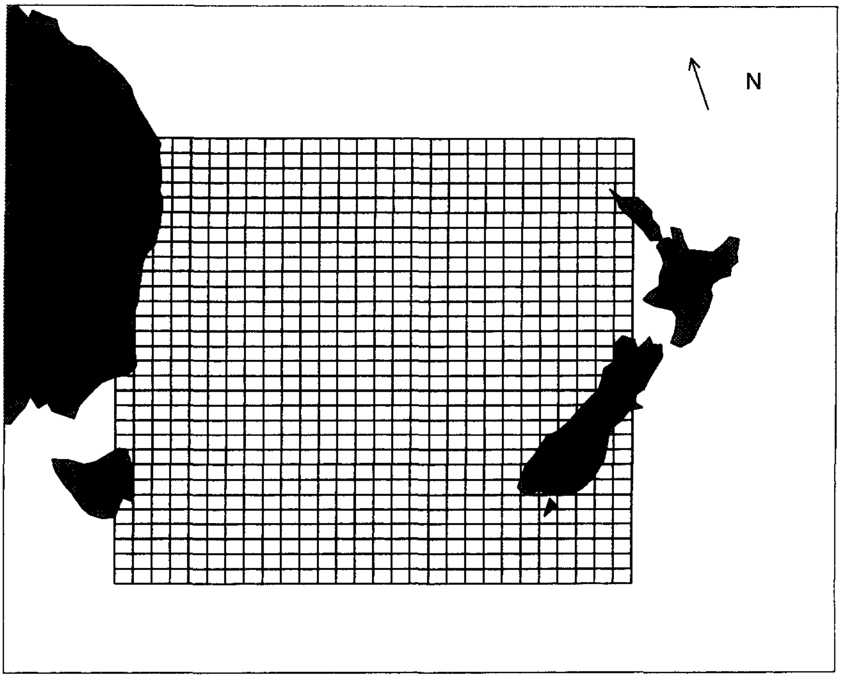

Fig. 3. The computational grid used for the one month hindcast of the Tasman Sea.

ution of 22.5°). Surface (10m) wind fields were obtained from the Australian Bureau of Meteorology atmospheric circulation model, RASP.

A one month hindcast for September, 1988 was performed. During this period a total of seventy (70) altimeter passes of GEOSAT occurred through the computational grid. The ground tracks of the satellite are shown in Fig. 4. On average, approximately two passes per day occurred through the computational grid (one ascending and one descending) with the accumulated ground track separation over the full month being approximately 100km.

Two runs were performed with the model, one without assimilation (henceforth termed the NOAS run) and one with assimilation (henceforth termed the AS run). Suitable in situ data to evaluate model performance were not available. Data from a number of sites along the east coast of Australia were investigated. These data are, however, close to land and in water of finite depth. The 70km spatial resolution of the model would be far too coarse to be reliable so close to land. In addition, as will be seen in later examples, the mean wave direction in the area is generally from west to east. Hence, changes to the model due to assimilation generally propagate towards the east and no significant changes are seen along the East coast of Australia.

To overcome the lack of in situ data, independent GEOSAT altimeter passes were used to evaluate model performance. This was achieved by comparing altimeter values of H_s for each pass with the model values along the pass, but before the data for the pass had been assimilated into the model. As the data for the pass under consideration has not been used by the assimilation scheme at that time, it is independent.

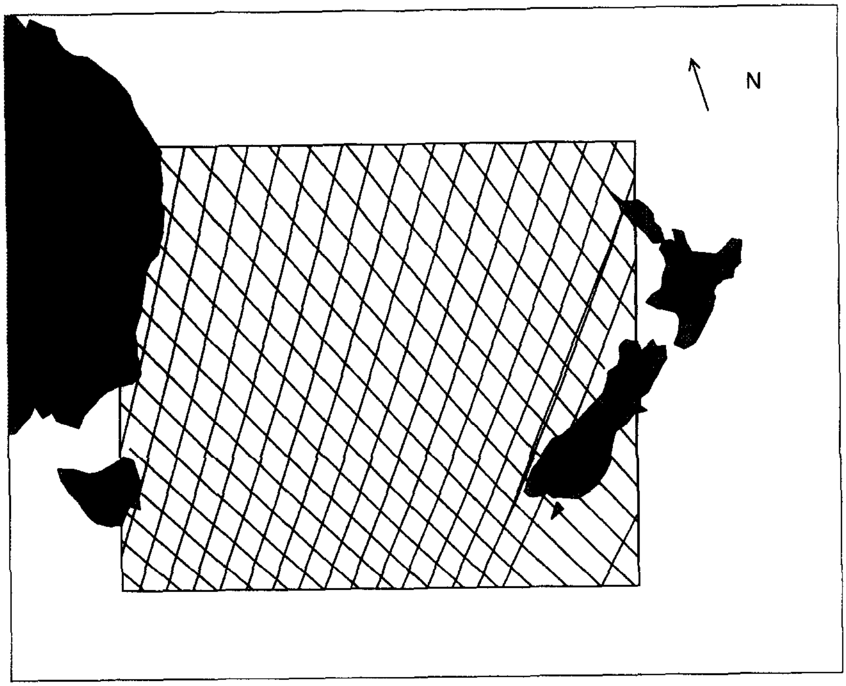

Fig. 4. Satellite ground tracks through the computational grid for the full period of the one month hindcast.

5.2. *Performance of assimilation scheme*

In order to assess model performance, the objective indicators of normalized *rms* error and *bias* were evaluated in the following manner:

$$rms = \sqrt{\frac{1}{N}\Sigma\varepsilon^2} \tag{16}$$

and

$$bias = \frac{1}{N}\Sigma\varepsilon \tag{17}$$

where the summations in (16) and (17) are over all the altimeter data points (N) of the full set of 70 passes during the simulation and

$$\varepsilon = \frac{H_s(model) - H_s(alt)}{H_s(alt)}. \tag{18}$$

In (18) $H_s(alt)$ is the altimeter value of significant wave height and H_s (*model*) is the corresponding model value. As the model and altimeter data do not correspond in space, the model data have been interpolated to the corresponding altimeter positions using bilinear interpolation.

Results for these two variables for the September, 1988 hindcast are shown in Table 1. The results in Table 1 show a 10% reduction in the *rms* error and a 33% reduction in the bias as a result of the assimilation scheme. These results show a substantial improvement in model performance. More insight into model performance can however be obtained by considering individual altimeter passes. The results from two such passes are considered below.

Figure 5 show the AS and NOAS results for the period between 14:00 16 Sept. 1988 and 14:00 17 Sept. 1988. An ascending altimeter pass occurs at 14:00 16 Sept. 1988 (Fig. 5a). The track passes along the southern coast of the south island of New Zealand, across the centre of the grid and exits on the northern boundary. As a result of the assimilation, values of H_s near the New Zealand coast have been increased by approximately 2.5m. In contrast, in the northern central region of the grid the assimilation has reduced H_s by approximately 1m (Fig. 5a). The mean wave direction near the New Zealand coast is towards the north–east and that in the northern central region of the grid toward the west–south–west. Comparison of Fig. 5a and 5b (period of 9 hours) clearly shows the difference fields in these two regions propagating in these respective directions. Both positive and negative changes to the wave field appear to persist in the model for significant periods.

At 00:30 17 Sept. 1988 (Fig. 5c) a descending altimeter pass occurs close to the coast of New Zealand and through the region corrected by the previous altimeter pass. Figure 6 shows the comparison between the measured altimeter data and the AS and NOAS runs along this ground track. In the region updated by the previous pass, the AS run is in far better agreement with the altimeter data than the NOAS run. Indeed, the AS run overestimates the wave energy. This is an indication that the region of influence ascribed to the altimeter data from the previous pass in the SI scheme was probably too large. As the pass is relatively close to the New Zealand coast this is most likely an indication that the region of influence decreases close to continental boundaries.

The data from this altimeter pass were assimilated into the model and Fig. 5c and 5d show that the difference field continues to propagate in the mean wave direction towards the north–east, partly impinging on the coast of the south island of New Zealand and partly propagating further to the north. An ascending altimeter pass occurs over this region at 14:00 17 Sept. 1988 (Fig. 5e). Figure 7 shows the comparison between AS, NOAS and altimeter data along this ground track. Along the region of this ground track near the eastern boundary of the grid (region to which changes from previous pass have propagated), the agreement between altimeter data and AS run are excellent and far better than the NOAS run. Further to the north, where there has been little influence from assimilated data the AS and NOAS runs are similar and both significantly underestimate H_s.

Table 1. Performance statistics for the AS and NOAS runs

	No Assimilation (NOAS) Run	Assimilation (AS) Run
rms	0.409	0.366
bias	-0.171	-0.114

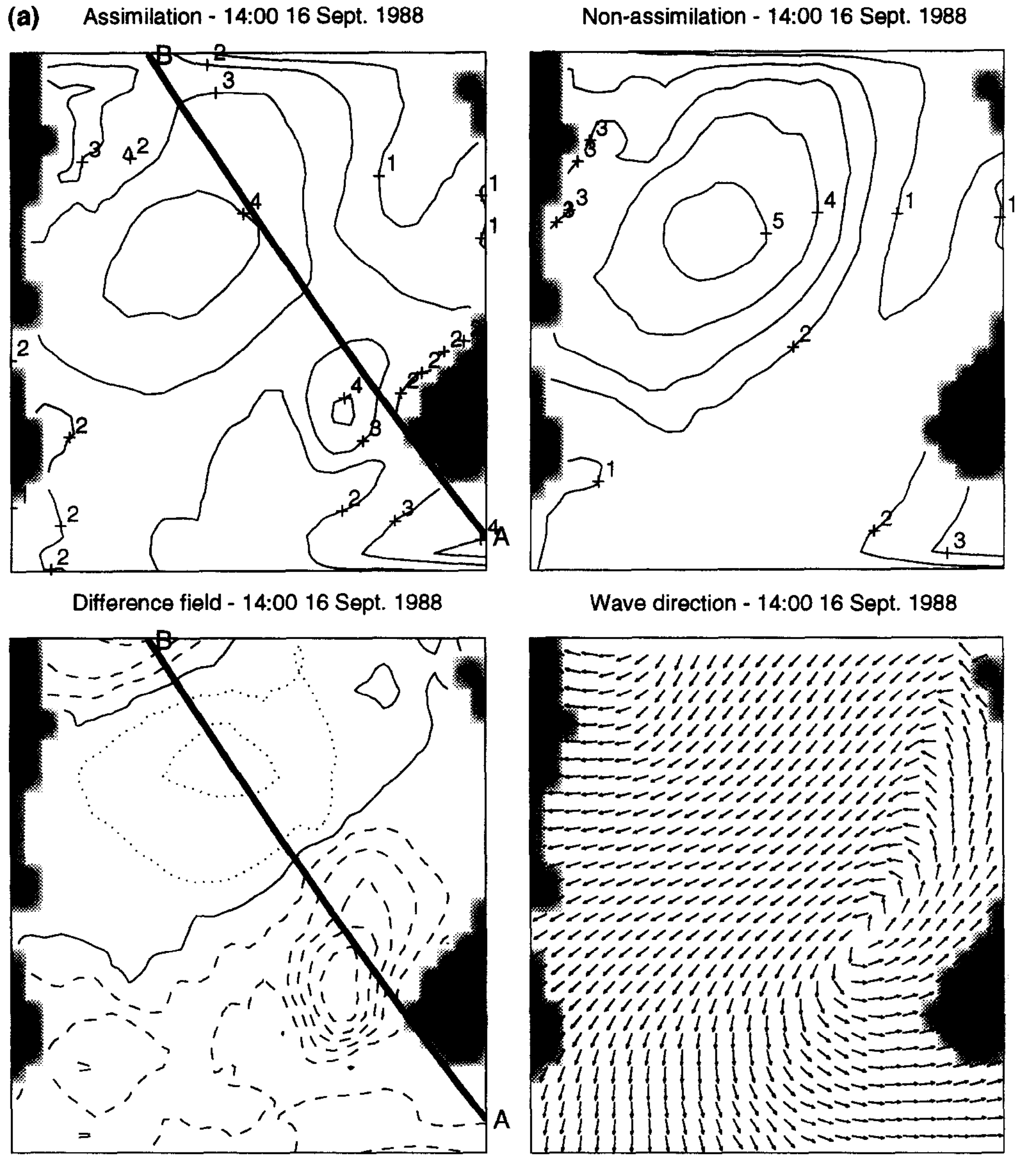

Fig. 5. Assimilation and No-assimilation results for the period between 14:00 16 Sept. 1988 and 14:00 17 Sept. 1988. The individual panels starting from the top left and proceeding in a clockwise fashion show: Contours of H_s for the AS run, Contours of H_s for the NOAS run, Mean direction of propagation (AS and NOAS); Contours of the difference field [ie. H_s(AS)$-H_s$(NOAS)]. The contour interval for the two H_s panels is 1m and the contour values are marked. For clarity, the contour values of the difference field are not shown. The contour interval, however, is 0.5m. The zero contour is shown with a solid line. Positive contours are marked with dashed lines whilst negative contours are marked with dotted lines. The ground tracks of altimeter passes are shown with a thick solid line at their times of occurrence. A letter A marks the point where the track enters the computational domain and a letter B where it leaves the domain. Thick dashed lines are used to show where an altimeter pass will occur at the next time step.

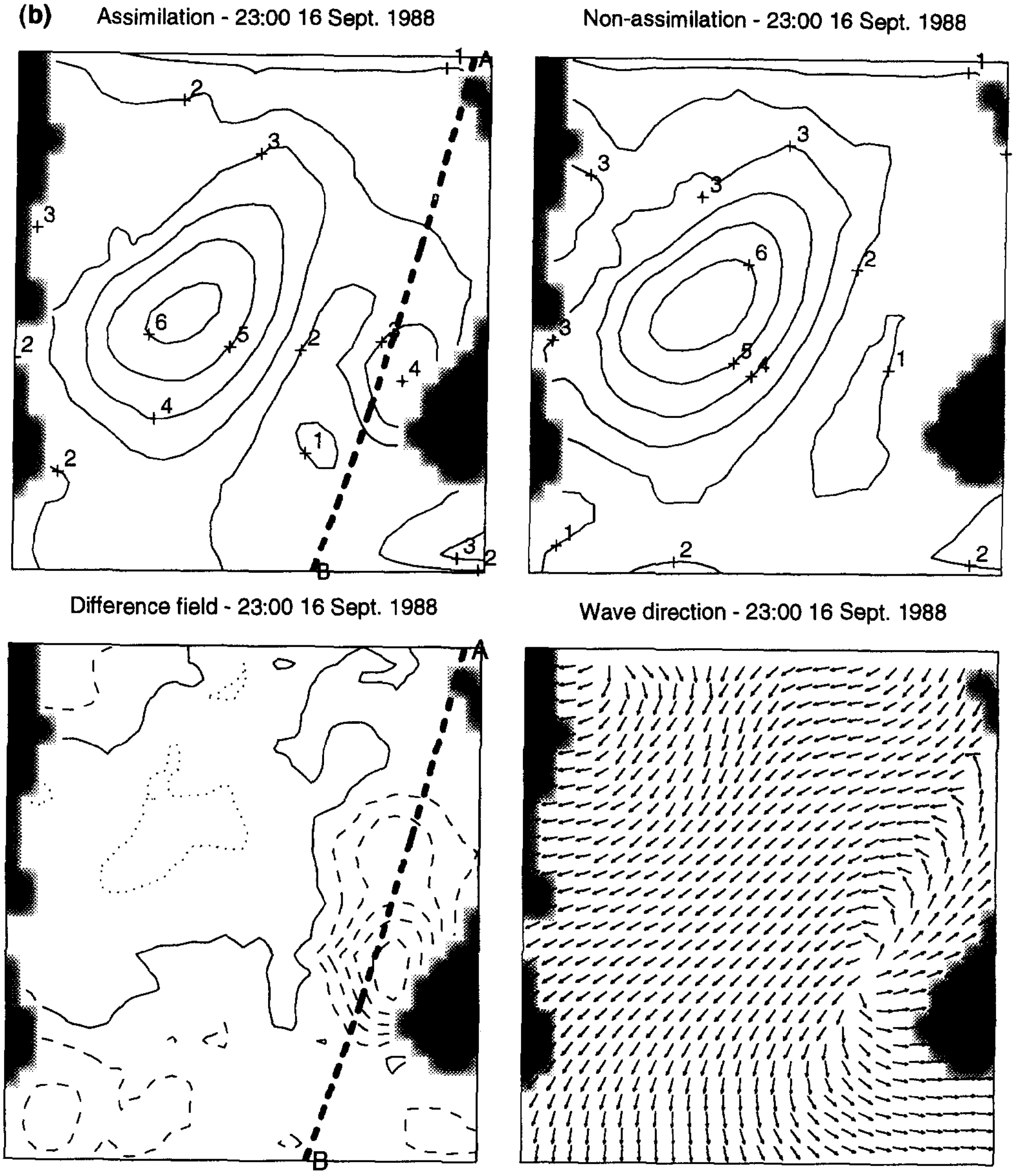

Fig. 5. Continued

6. CONCLUSIONS

This paper has presented a data assimilation scheme suitable for a second generation wave model. This contrasts with recent data assimilation attempts which have concentrated on applications for third generation models (Janssen *et al.*, 1989; Lionello *et al.*, 1992; Bauer *et al.*, 1990, 1992a). The use of such a relatively simple model is justified for the following reasons:

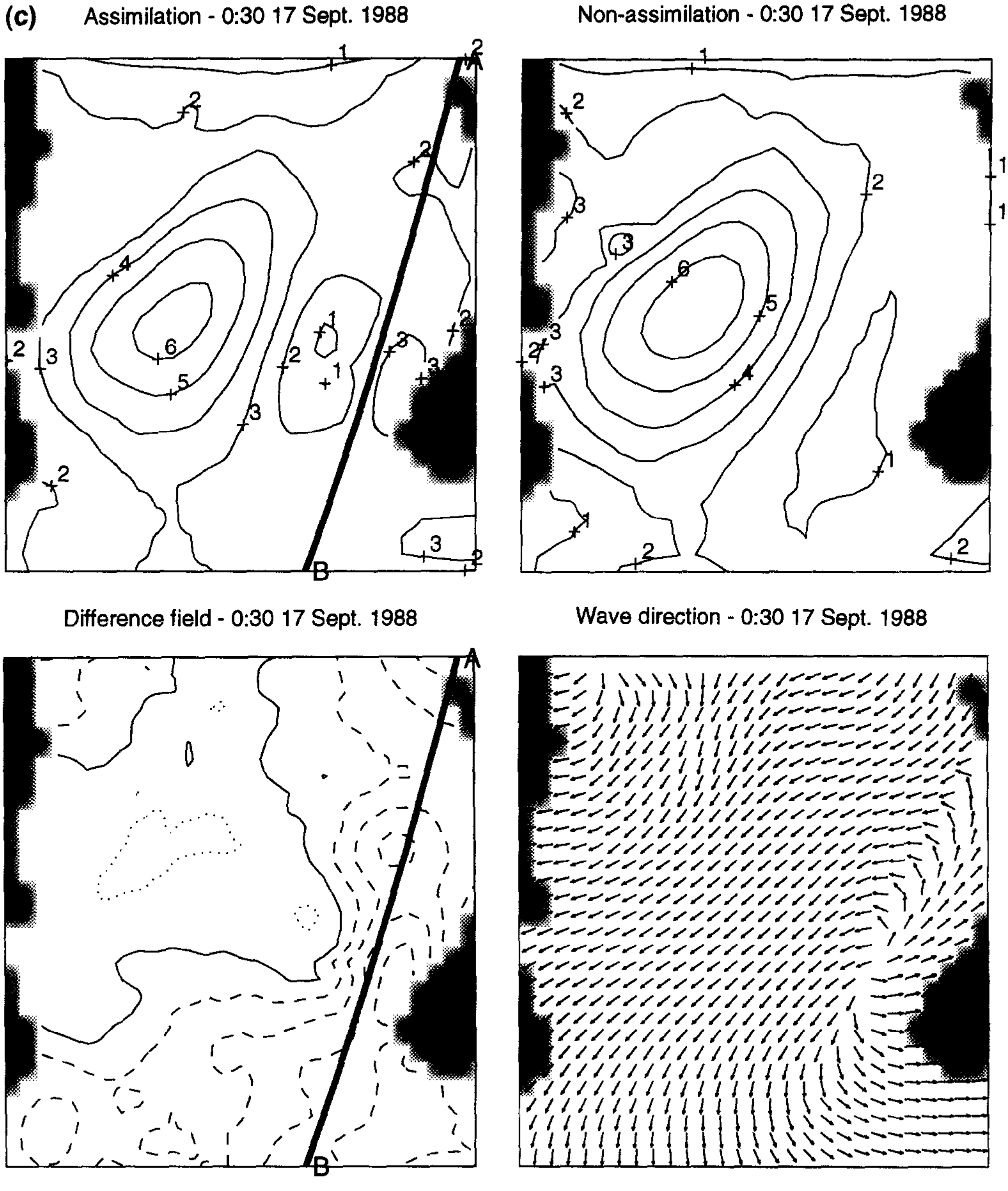

Fig. 5. Continued

(1) Second generation models are computationally far less expensive and hence require only modest computational resources. For many engineering applications the expense of a third generation model is not justified.
(2) We concentrate here on hindcast applications. Provided the assimilation scheme is successful, the sophistication of the model physics becomes less important. In such applications the assimilated data will mean that there should be little difference in performance between second and third generation models.

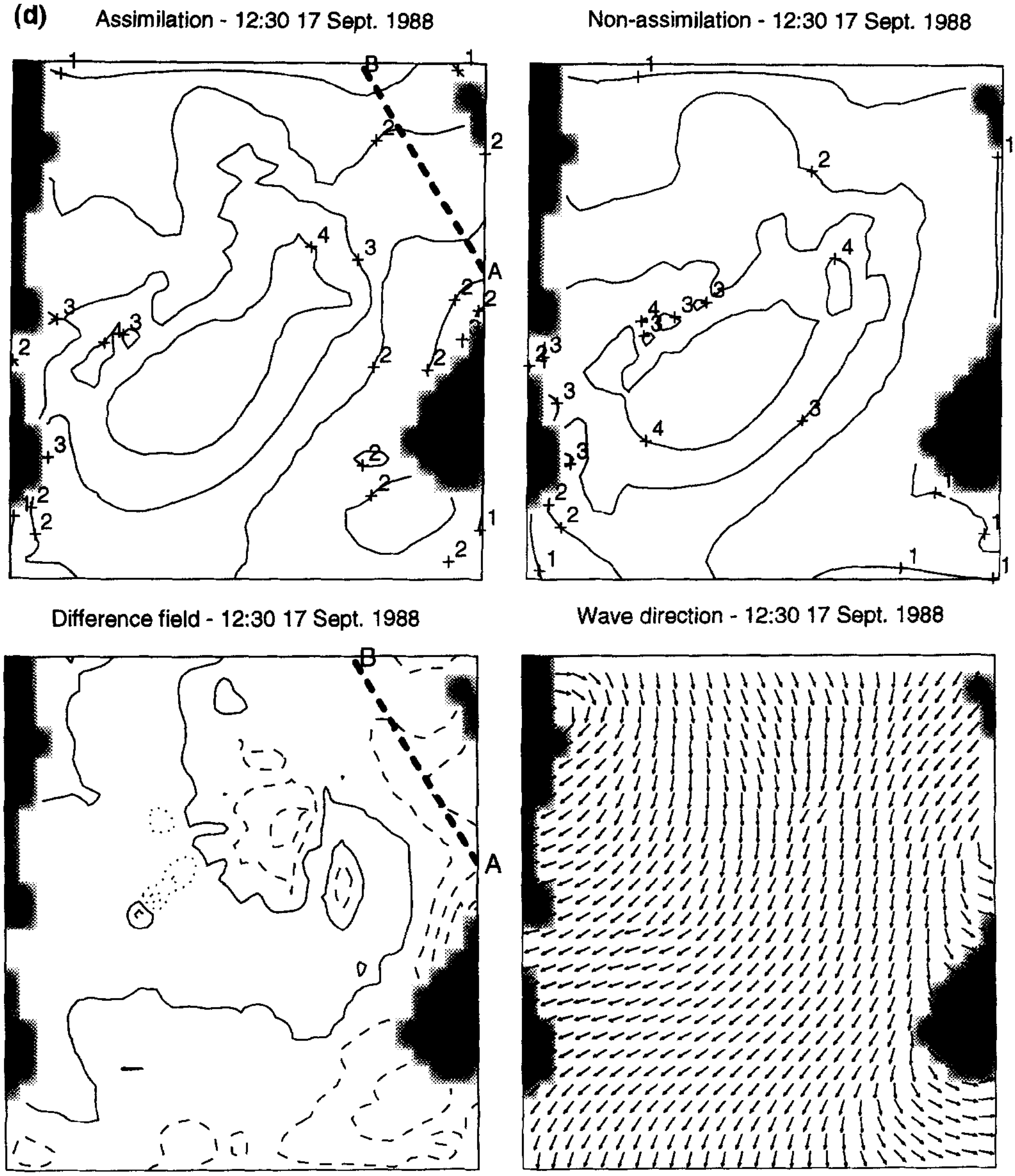

Fig. 5. Continued

The scheme adopted here recognizes that purely *ad hoc* changes cannot be made to the spectrum in a dynamic spectral wave model. Any spectral changes must be in equilibrium with the imposed wind field. A scheme has been presented which achieves such changes for the case where the observed data to be assimilated is in the form of altimeter observations of significant wave height, H_s.

In contrast to previous wave model assimilation schemes a statistical interpolation (SI) scheme has been adopted. This scheme provides a statistical rationale for extending the

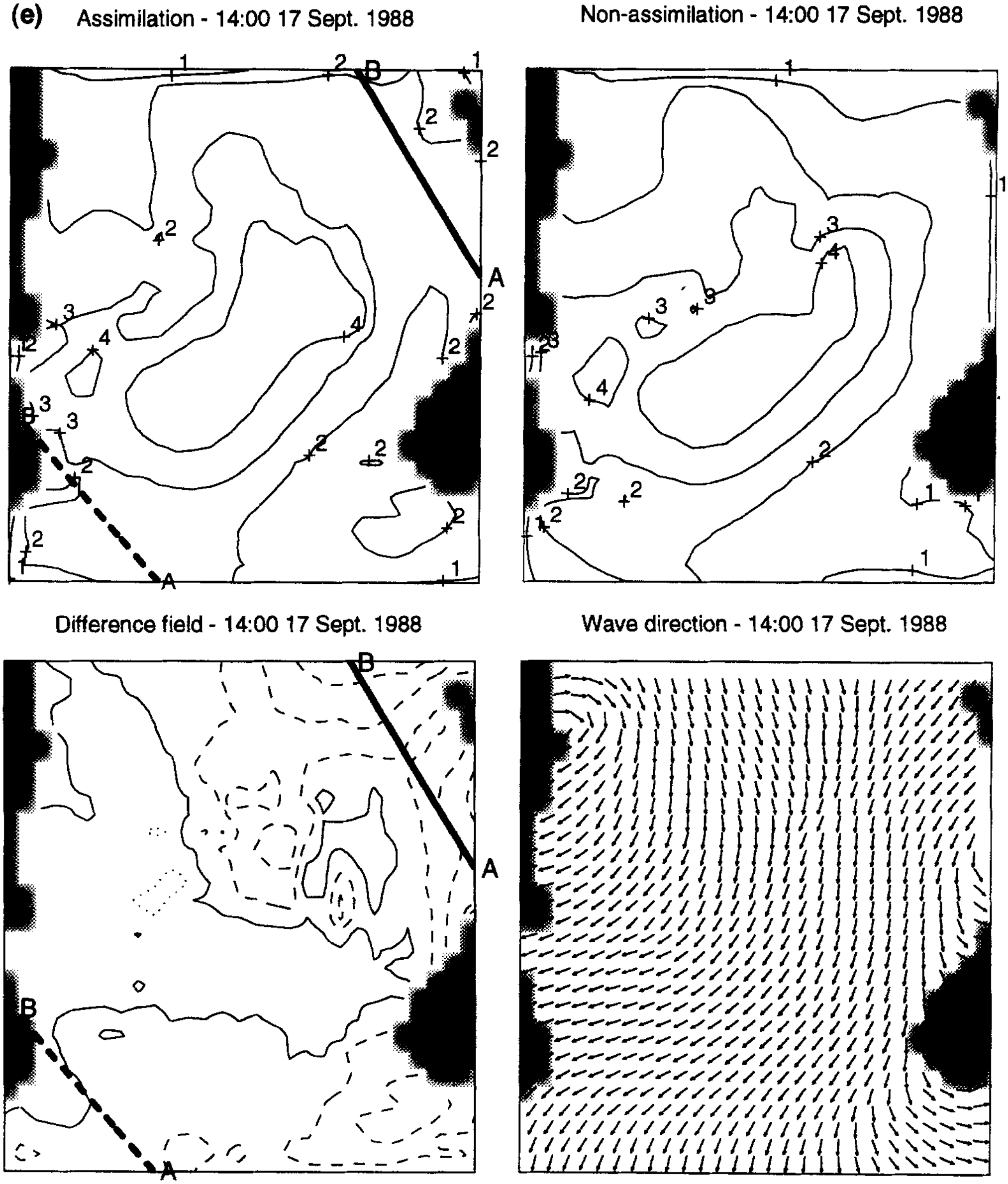

Fig. 5. Continued

region of influence of altimeter observations to areas adjacent to the satellite ground track. Previous applications have applied simple 'blending' schemes with *ad hoc* assumptions as to the extent to which the altimeter observations can be applied to adjacent regions.

Results from a one month hindcast for the Tasman Sea show a significant improvement in model performance as a result of the application of the assimilation scheme. Corrections to the wave field persist within the model and propagate in the mean wave direction.

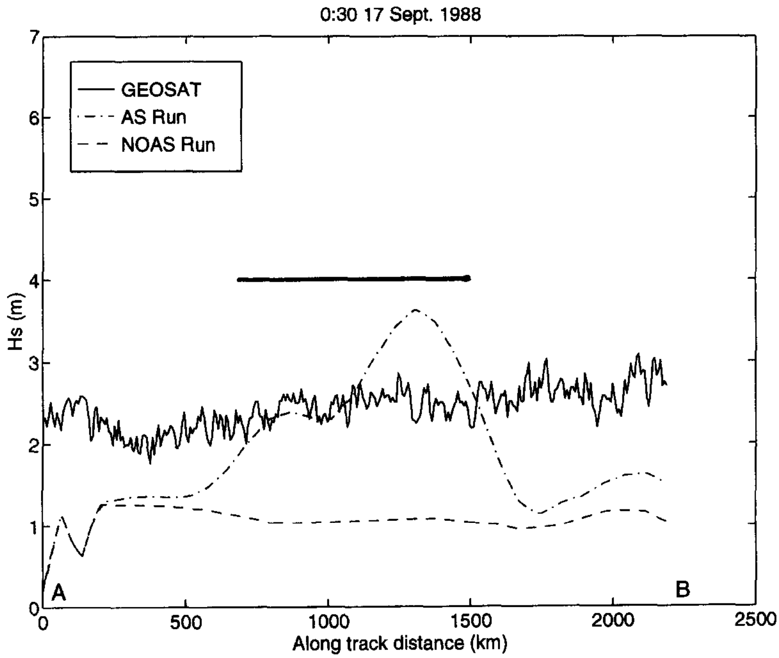

Fig. 6. Comparison between the AS, NOAS and observed altimeter values of H_s along the altimeter ground track at 00:30 17 Sept. 1988. The region influenced by the previous altimeter pass is shown by the thick horizontal line. The points marked A and B corresponds to the similarly labeled points on the ground track in Figure 5c.

Independent altimeter observations show that these updated wave fields decay at the appropriate rates and produce accurate updates to the 'downstream' wave field.

Further work is underway to accurately determine spatial correlations for observed data for use in the SI scheme. The results suggest that the spatial correlation of observations decreases with proximity to the coast. In addition, it is highly likely that they vary with latitude and possibly seasonally.

Although model performance is improved by assimilation, the relatively large distance between ground tracks for a single satellite means that significant regions of the grid are unaffected by the process. Multiple orbiting platforms would solve this problem and the increase in data would be expected to greatly improve model results.

REFERENCES

Barnett, T.P. 1968. On the generation, dissipation and prediction of ocean wind waves. *J. Geophys. Res.* **73**, 513–528.

Bauer, E., Hasselmann, S., Young, I.R. & Hasselmann, K., Data Assimilation into a Wave Prediction Model, 25th General Assembly of the European Geophysical Society, Copenhagen, 1990, 23–27 April.

Bauer, E., Hasselmann, K. & Young, I.R., Satellite Data Assimilation in the Wave Model 3G-WAM, Proc. Central Symposium of the 'International Space Year', Munich, Germany, 1992a, March 30–April 4, 377–380.

Bauer, E., Hasselmann, S. and Hasselmann, K. 1992. Validation and assimilation of Seasat altimeter wave heights using the WAM wave model. *J. Geophys. Res.* **97**, 12671–12682.

De Valk, C.F. and Calkoen, C.J., Wave data assimilation in a 3rd generation wave model for the North Sea–An optimal control approach, Delft Hydraulics report X38, 1989, Delft.

Ewing, J.A. 1971. A numerical wave prediction method for the North Atlantic Ocean. *Deutsche. Hydr. Zeit.* **24**, 241–261.

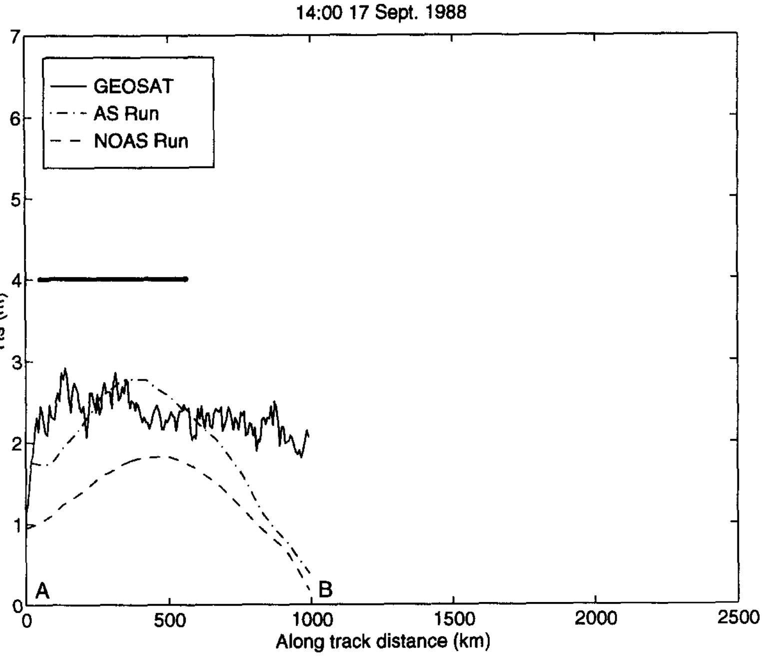

Fig. 7. Comparison between the AS, NOAS and observed altimeter values of H_s along the altimeter ground track at 14:00 17 Sept. 1988. The region influenced by the previous altimeter pass is shown by the thick horizontal line. The points marked A and B corresponds to the similarly labeled points on the ground track in Figure 5e.

Gandin, L.S. 1963. *Objective analysis of meteorological fields*, Gidrometeoizdat, Leningrad, (Translated from Russian by The Israeli Program for Scientific Translations, 1965), 1963, 242pp.

Gelci, R., Cazalé, H. and Vasal, J. 1957. Prévision de la houle. La méthode des densités spectroangularires. *Bull. Inform. Comité Central Oceanogr., D'Etude Côtes* **9**, 416–435.

Hasselmann, K., Hasselmann, S., Bauer, E., Brüning, C., Lehner, S., Graber, H.C. & Lionello, P., Development of a satellite SAR image spectra and altimeter wave height data assimilation system for ERS-1, Final Report ESA Study Contract No. 6875/87/HGE-I(SC), Max-Planck-Institut für Meteorologie, Report No. 19, 1988, 155pp.

De Las Heras, M.M. and Janssen, P.A.E.M. 1992. Data assimilation with a coupled wind-wave model. *J. Geophys. Res.* **97**, 20261–20270.

Janssen, P.A.E.M., Komen, G.J. and De Voogt, W.J.P. 1984. An operational coupled hybrid wave prediction model. *J. Geophys. Res.* **89**, 3635–3654.

Janssen, P.A.E.M., Lionello, P., Reistad, M. and Hollingsworth, A. 1989. Hindcasts and data assimilation studies with the WAM model during the SEASAT period. *J. Geophys. Res.* **94**, 973–993.

Komen, G.J. 1985. Introduction to wave models and assimilation of satellite data in wave models, In: The use of satellite data in climate models. *Proc. Alpbach Conference, ESA Publ., ESA SP* **244**, 21–26.

Le Dimet, F.-X. and Talagrand, O. 1986. Variational algorithms for analysis and assimilation of meteorological observations: Theoretical aspects. *Tellus* **38A**, 97–110.

Lionello, P., Günther, H. and Janssen, P.A.E.M. 1992. Assimilation of altimeter data in a global third generation wave model. *J. Geophys. Res.* **97**, 14253–14474.

Lorenc, A. 1981. A global three-dimensional multivariate statistical interpolation scheme. *Mon. Weath. Rev.* **109**, 701–721.

Marchuk, G.I. 1974. *The numerical solution of problems of atmospheric and oceanic dynamics*, Gidrometeoizdat, Leningrad, (Translated from Russian by Rainbow Systems Inc., Alexandria, Virginia), 1974, 387pp.

Phillips, O.M. 1958. The equilibrium range in the spectrum of wind-generated waves. *J. Fluid. Mech.* **4**, 426–434.

Schnabel, R.B. and Eskov, E. 1990. A new modified Cholesky factorization. *AIAM J. Sci. Stat. Comput.* **11**, 1136–1168.

Thomas, J.P. 1988. Retrieval of energy spectra from measured data for assimilation into a wave model. *Q.J.R. Meteorol. Soc.* **114**, 781–800.
Young, I.R. 1988. A Shallow Water Spectral Wave Model. *J. Geophys. Res.* **93**, 5113–5129.

APPENDICES

A STATISTICAL INTERPOLATION BASIS

The mathematical description of statistical interpolation used here, follows very closely that of Lorenc (1981), but is nevertheless presented in some detail for completeness.

Let

$$a = A - T, b = B - T, p = P - T \tag{A1}$$

denote deviations of analyzed, observed, and predicted (first guess) values from the 'true' value respectively, and

Let

$$E^a = <a^2>^{1/2}, E^0 = <b^2>^{1/2}, E^p = <p^2>^{1/2} \tag{A2}$$

denote their associated error estimates.

The corresponding dimensionless values are now defined

$$\alpha = a/E^a, \beta = b/E^0, \pi = p/E^p$$
$$q = (B - P)/E^p, r = (A - P)/E^p$$
$$\varepsilon^0 = E^0/E^p, \varepsilon^a = E^a/E^p \tag{A3}$$

All the above take subscripts i (or j) ranging over all observed values, or k ranging over all analyzed values, whatever their position.

The basis of the statistical interpolation method is that the analyzed deviation from the prediction is given by a linear combination of N observed deviations

$$r_k = \sum_{i=1}^{N} w_{ik} q_i \tag{A4}$$

with the weights (w) determined so as to minimize the estimated analysis error E_k^a.

After appropriate substitution for r_k and q_i

$$\alpha_k \varepsilon_k^a = \pi_k + \sum_{i=1}^{N} w_{ik}(\beta_i \varepsilon_i^0 - \pi_i) \tag{A5}$$

Squaring this and taking the ensemble average gives

$$\begin{aligned}(\varepsilon_k^a)^2 = 1 + 2 \sum_{i=1}^{N} w_{ik}(<\pi_k \beta_i> \varepsilon_i^0 - <\pi_k \pi_i>) \\ + \sum_{i=1}^{N} \sum_{j=1}^{N} w_{ik} (<\pi_i \pi_j> + \varepsilon_i^0 <\beta_i \beta_j> \varepsilon_i^0 \\ - \varepsilon_i^0 <\beta_i \pi_j> - <\pi_i \beta_j> \varepsilon_j^0) w_{jk}\end{aligned} \tag{A6}$$

using vector and matrix notation:

$$\mathbf{w}_k = [w_{ik}] \tag{A7}$$

$$\mathbf{h}_k = [<\pi_k \pi_i> - <\pi_k \beta_i> \varepsilon_i^0] \tag{A8}$$

$$\mathbf{q} = [q_i] \tag{A9}$$

$$\mathbf{M} = [<\pi_i\pi_j> + \varepsilon_i^0<\beta_i\beta_j> \varepsilon_j^0 - \varepsilon_i^0<\beta_i\pi_j> - <\pi_i\beta_j> \varepsilon_j^0] \tag{A10}$$

Equations A5 and A6 become

$$r_k = \mathbf{w}_k^T\mathbf{q} \tag{A11}$$

$$(\varepsilon_k^a)^2 = 1 - 2\mathbf{w}_k^T\mathbf{h}_k + \mathbf{w}_k^T\mathbf{M}\mathbf{w}_k \tag{A12}$$

for which the least squares solution gives

$$\mathbf{w}_k = \mathbf{M}^{-1}\mathbf{h}_k \tag{A13}$$

Thus, the analyzed value and estimated error corresponding to these weights are

$$r_k = \mathbf{h}_k^T\mathbf{M}^{-1}\mathbf{q} \tag{A14}$$

$$(\varepsilon_k^a)^2 = 1 - \mathbf{h}_k^T\mathbf{M}^{-1}\mathbf{h}_k \tag{A15}$$

since $\mathbf{M}^{-1}$ and $\mathbf{q}$ are independent of the point being analyzed, the weights w_k do not have to be explicitly calculated for grid-point analysis computation. Instead from A14 it can be written

$$\mathbf{c} = \mathbf{M}^{-1}\mathbf{q} \tag{A16}$$

$$r_k = \mathbf{c}^T\mathbf{h}_k \tag{A17}$$

Terms $< \pi_i\pi_j >$ in A10 are usually called error correlations and $< p_ip_i >$ covariances, although this is only true if the biases $< p_i >$ are zero. This is not strictly necessary for the above derivation, but if it doesn't happen A4 is not the best interpolation equation. It is also usual to neglect the correlations between prediction error and observation error, that is to assume $< \pi_i\beta_i > = 0$. If an observation type, however, is used for which these correlations are known to be non-zero, then their inclusion is straight-forward.

As SI combines first-guess and observed data according to estimated accuracy of each, specification of reasonable estimates for prediction and observational errors is vital to the correctness of the results. What is desired of the first-guess field is that it is the best available prior estimate. This may often be a short range forecast, but need not necessarily be so (it could be climatology, or a previous analysis, if no forecast is available).

The above shows, that a practical application of SI should include at least the following steps:

(1) provision of a first-guess field at all grid-points and all observational points, which is usually a short range forecast;
(2) modelling of the prediction error correlations $< \pi_i\pi_j >$;
(3) modelling of the observational error correlations $< \beta_i\beta_j >$;
(4) selection of observations to influence analyzed (grid) point values;
(5) solution of the system of linear equations to obtain the interpolation weights.

B. APPLICATION OF STATISTICAL INTERPOLATION TO DATA CHECKING

The application of SI to data checking by cross-validation minimizes the expected variance of the difference between analyzed and observed deviations from the prediction, i.e. the term

$$<(r_k - q_k)^2> = (\varepsilon_k^0)^2 + 1 - 2\mathbf{w}_k^T\mathbf{M}_k + \mathbf{w}_k^T\mathbf{M}\mathbf{w}_k \tag{A18}$$

instead of the terms in A6.

If the observation being checked is also used for the interpolation then $\mathbf{M}_k$ is a column of $\mathbf{M}$ and minimizing A18 leads to the trivial result

$$\mathbf{w}_k = \mathbf{d}_k \tag{A19}$$

where $\mathbf{d}_k$ is defined as a vector whose k[th] element is one and whose other elements are zero. Since we are trying to interpolate a value for an observation including its observational error, the best value is naturally the observation itself.

However, A18 is to be minimized with constraints that observation k and other 'suspect' and already rejected observations have zero weights.

If l_m (m=1 to n) is a list of these observations, the constraints can be written

$$\mathbf{d}_{lm}^{T}\mathbf{w}_k = 0 \text{ (for } m = 1, n) \tag{A20}$$

Minimizing A18 subject to these constraints gives

Substituting A27 into A11 gives the equivalent of A16

$$\mathbf{c} = \mathbf{M}^{-1}\mathbf{q} - \mathbf{M}^{-1}\mathbf{D}(\mathbf{D}^T\mathbf{M}^{-1}\mathbf{D})^{-1}\mathbf{D}^T\mathbf{M}^{-1}\mathbf{q}$$

$$(\varepsilon_k^a)^2 = 1 - \mathbf{h}_k^T\mathbf{w}_k = 1 - \mathbf{h}_k^T\mathbf{U}\mathbf{h}_k \tag{A28}$$

and the estimated analysis error corresponding to weights w_k is

$$(\varepsilon_k^a)^2 = 1 - \mathbf{h}_k^T\mathbf{w}_k = 1 - \mathbf{h}_k^T\mathbf{U}\mathbf{h}_k \tag{A29}$$

where

$$\mathbf{U} = \mathbf{M}^{-1} - \mathbf{M}^{-1}\mathbf{D}(\mathbf{D}^T\mathbf{M}^{-1}\mathbf{D})^{-1}\mathbf{D}^T\mathbf{M}^{-1} \tag{A30}$$

Imposing zero constraints on the weights instead of excluding constrained observations from the covariance matrix plays a key role in reducing computing time since it allows the use of the same matrix inversion repeatedly for the whole analysis domain for both data checking and analysis, the latter including analysis error estimation.